J Therm Anal Calorim (2012) 109:373–379
DOI 10.1007/s10973-011-1698-z

Structural and thermal characterization of sodium ibandronate monohydrate

Luciana Malpezzi · Elisabetta Maccaroni · Giordano Carcano · Gianpiero Ventimiglia

Received: 22 September 2010 / Accepted: 24 May 2011 / Published online: 10 June 2011

Abstract Sodium Ibandronate (NaIb) belongs to the nitrogen-containing bisphosphonates drugs, used as anti-resorptive medications for the treatment of osteoporosis. The crystalline form of NaIb monohydrate was observed to undergo reversible thermal dehydration and rehydration, according to its hygroscopic nature and to the arrangement of the water molecules in the crystal lattice. Dehydration and rehydration were observed and confirmed by variable temperature X-ray diffraction on the basis of the DSC pattern and TG analysis that shows, by heating the sample from 40 to 200 °C, a loss of 5% weight corresponding to a water molecule loss. The water loss causes a phase transition to a more dense phase that can be rehydrated if it is left in a humid environment. The solid state characterization of NaIb monohydrate has been performed by X-ray single crystal diffraction analysis. The NaIb crystallizes as monohydrate salt in the triclinic system, space group P-1, with $Z = 2$, $a = 5.973(1)$ Å, $b = 9.193(1)$ Å, $c = 14.830(2)$ Å, $\alpha = 98.22(1)°$, $\beta = 98.97(1)°$, $\gamma = 93.74(1)°$, $V = 792.9(2)$ Å^3. Each anionic group exist as zwitterionic entity with a total charge of -1. In the crystal packing, the octahedral coordination around the Na cations determines a centrosymmetric double chains structure elongated into the [100] direction. The water molecules are located inside the inter-chains cavities.

Keywords Sodium ibandronate · X-ray analysis · Thermal analysis · Structure determination

L. Malpezzi (✉) · E. Maccaroni
Department of Chemistry, Materials and Chemical Engineering "G. Natta", Via Mancinelli 7, 20131 Milano, Italy
e-mail: luciana.malpezzi@polimi.it

G. Carcano
CNR-IENI—Sezione di Lecco, Corso Promessi Sposi 29, 23900 Lecco, Italy

G. Ventimiglia
Chemessentia srl—Chemo Group, Via Bovio 6, 28100 Novara, Italy

Introduction

Sodium Ibandronate (NaIb) [3-(*N*-methyl-*N*′-pentyl)-amino-1-hydroxypropane-1,1-diphosphonic acid monosodium salt] belongs to the nitrogen-containing bisphosphonates, a class of drugs used in the prevention and treatment of osteoporosis and similar diseases, which has been subjected to many pharmacological [1–3] and structural studies [4–8], in order to explore the structural basis of their activity against bone diseases and against some parasite replication. The sodium salts of the bisphosphonates compound show a further interest due to their better solubility and bio-availability.

The bone is a living dynamic structure which constantly undergoes a process of bone resorption (breakdown) and bone formation. When this process of remodelling, or bone turnover, removes more bone than it replaces, osteoporosis results, increasing the risk of fracture. The bisphosphonates, by virtue of their P–C–P backbone structure which acts as inhibitor of the destructive phase of bone turnover (resorption), are currently the most effective anti-resorptive medications. Their anti-resorptive potency is influenced by the chemical and three-dimensional structure of the side chain attached to the central carbon of the P–C–P backbone and the presence of a nitrogen-containing group, at a critical distance from the carbon atom, has been know to increase the strength of the drug [9]. Sodium Ibandronate, a nitrogen-containing bisphosphonate derivative characterized by an aliphatic tertiary amine side chain (see Scheme 1), directly

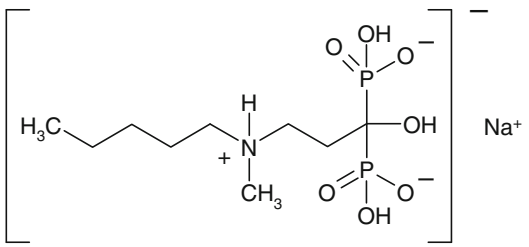

Scheme 1 Schematic drawing of NaIb

inhibits osteoclast activity, presenting a pharmacologic alternative for controlling hypercalcemia. NaIb binds to hydroxyapatite in calcified bones, rendering them resistant to hydrolytic dissolution by phosphatases, thereby inhibiting both normal and abnormal bone resorption. This drug increases bone mass and decreases the risk of fractures and it is therefore particularly adapted to bone diseases and calcium metabolic disorders such as osteoporosis, osteolysis, Paget's disease, Bechterew's disease, bone metastases, urolithiasis and for the prevention of heterotrophic ossifications. Due to its influence on calcium metabolism, it also forms a basis for the treatment of rheumatoid arthritis, osteoarthritis and degenerative arthrosis.

The patent literature reports the characterization by X-ray powder diffraction, IR and Raman spectroscopy of several polymorphic forms of the title compound [10–12]. The same API, in different solid arrangements, may show different stability, solubility, bio-availability and adsorption from the tissues or biological membrane, thus heavily influencing pharmaceutical performance. Thus, a complete molecular and structural characterization obtained from diffractometric techniques, coupled with ancillary information derived from thermal analyses or solid state NMR, is highly favourable in most cases in the pharmaceutical field [13–16]. Accordingly, we present here the structural characterization and thermal behaviour of NaIb monohydrate (Fig. 1), since a complete characterization of solid NaIb, such as the molecular and crystalline structure, obtained from single crystal X-ray analysis and the thermal properties, is still absent.

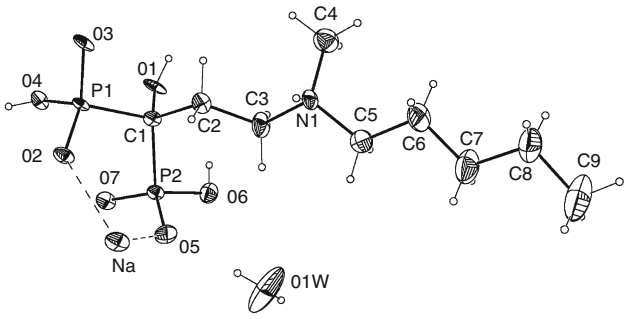

Fig. 1 A view of the asymmetric unit of title compound, showing the atom labelling scheme

Experimental

Materials

Sodium Ibandronate monohydrate was synthesized reacting ibandronic acid [17] with sodium hydroxide affording the corresponding monosodium salt, which is isolated as 2-propanol hemisolvate and hemihydrated adduct. Finally, crystallization from a water/acetone binary mixture leads to NaIb, monohydrated adduct, as crystalline powders.

Methods

Thermal analysis

Differential scanning calorimetry was performed on a Perkin Elmer DSC 8500 instrument, purged with Nitrogen gas (purge: 20 mL min^{-1}). The system was calibrated with Indium (melting point 156.60 °C, heat of fusion 26.45 J g^{-1}). A few samples, enclosed in crimped aluminium pans and accurately weighted (from 3.100 to 5.453 mg), were heated at a scan rate of 10 °C min^{-1} from 40 to 200 °C.

Thermogravimetric analysis was carried out on a SEIKO TG/DTA 6200 Instrument. Two samples of NaIb monohydrate, of 5.031 and 5.374 mg, respectively, were heated in an alumina cell in the range 30–920 °C, under an Ar/air purge (flow rate of 100 mL min^{-1}) at a scan rate of 10 °C min^{-1}.

Single crystal X-ray diffraction analysis

A single crystal of NaIb monohydrate, 0.67 × 0.25 × 0.02 mm in size, obtained from slow evaporation of the recrystallization solution, was selected for X-ray measurements. Intensities data were collected, at room temperature, on a Bruker SMART APEX area detector diffractometer with a 5-cm crystal-to-detector distance and graphite-monochromatised Mo-Kα radiation (λ = 0.71069 Å) at 50 kV and 30 mA. A total of 8206 reflections (2212 unique, $R_{int} = 0.058$) was collected in the θ range 1.4–23.5°, corresponding to 99.9% of completeness in theta. Raw intensity data were corrected for absorption using SADABS v. 2.10 program (Sheldrick [18]).

Crystal data: $C_9H_{22}NO_7P_2Na{\cdot}H_2O$, $M_W = 359.22$ g mol^{-1}, triclinic, space group P-1, $a = 5.973(1)$ Å, $b = 9.193(1)$ Å, $c = 14.830(2)$ Å, $\alpha = 98.22(1)°$, $\beta = 98.97(1)°$, $\gamma = 93.74(1)°$, $V = 792.9(2)$ $Å^3$, $Z = 2$, $D_c = 1.505$ g cm^{-3}, F(000) = 380.

The structure was solved by direct methods using SIR97 program [19] which revealed the position of all non-H

atoms. The refinement was carried out on F^2 by full-matrix least-squares procedure with SHELXL97 [20] for 212 parameters, with anisotropic temperature factors for non-H atoms. The final stage converged to $R = 0.0588$ ($R_w = 0.1496$) for 1723 observed reflections (with $I \geq 2\sigma(I)$), and $R = 0.0774$ for all reflections. The hydroxyl and the amine H atoms were freely and isotropically refined, all other H atoms were placed in geometrically calculated positions and refined in a riding model. Crystallographic data have been deposited at the Cambridge Crystallographic Data Centre, with the deposition number: CCDC 792728.

Variable temperature X-ray powder diffraction

The X-ray powder diffraction pattern (XRPD) was collected at room temperature on an Ital-Structure θ/θ diffractometer, under the following condition: Ni-filtered Cu-Kα radiation ($\lambda = 1.5418$ Å); range $3° \leq 2\theta \leq 40°$; scan 0.04°; $t = 2$ s step^{-1}. The XRPD pattern was also calculated from the atomic coordinated determined by single crystal X-ray analysis. The experimental and calculated patterns are in complete agreement in the sequence of the diffracted peaks position thus resulting in describing the same crystalline phase. Some variations in the corresponding peak intensities is due to preferred orientation effects, a phenomenon frequently observed during data collection of organic powders compounds with anisotropic morphology.

The XRPD at non-ambient temperature were collected on a X'Pert PRO (PANanalytical) diffractometer equipped with an X'Celerator X-Ray detector and a thermal chamber (Anton Paar TTK 450) in the following conditions: Nickel filtered Cu-Kα radiation ($\lambda = 1.5418$ Å); range $3° \leq 2\theta \leq 40°$; slits system on incoming rays: Soller 0.04 rad, mask fixed 10 mm.

The powder of NaIb monohydrate, placed into the sample holder, was progressively heated in successive steps (25, 70, 110, 140, 155 and 180 °C) and maintained in isothermal conditions for about 10 min at each step, before and during data collection. A new crystalline phase has been observed at 155 °C. The first well defined peaks of the diffraction pattern of this new phase were selected for the indexing procedure using TOPAS program [21] allowing the determination of the approximate cell parameters (lattice constants).

Results and discussion

Thermal analysis

DSC experiments were carried out on a few samples and in all of them the DSC trace exhibits a broad endothermic curve starting at about 140 °C with the maximum of the peak at about 167 °C ($\Delta H = 42.2$ kJ mol^{-1}) (Fig. 2).

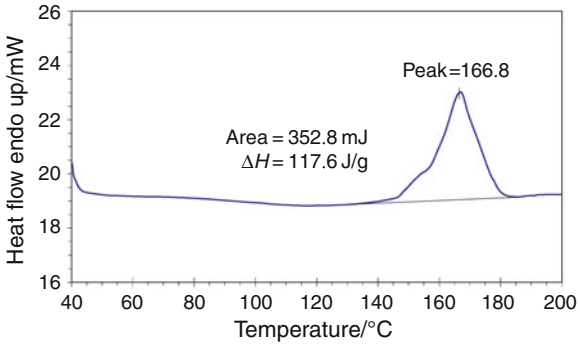

Fig. 2 DSC curve of NaIb monohydrate measured at 10 °C min^{-1}

After 220 °C, the sample was observed to undergo degradation, as shown by a deflection of the baseline (not reported). A peculiar feature of the endotherm is the presence of a shoulder in the low-temperature side of the curve. In order to investigate this aspect of the thermal behaviour of the drug, variable temperature X-ray powder diffraction analysis was undertaken (see infra). Furthermore, a thermogravimetric analysis was carried out (Fig. 3). Since the compound is known to be highly hygroscopic, two samples were first heated in an oven for 15 min at 60 °C and 5 min at 80 °C, respectively, and then measured by thermogravimetry, in order to remove potential surface water. Both measurements show the same weight loss of about 5% which corresponds to the release of one molecule of crystallized water per NaIb molecule. This result suggests that the shoulder observed on the DSC pattern is due to a phase transition into a new phase, due to the dehydration of the compound. The new formed phase appears to melt around 167 °C.

Single crystal X-ray diffraction

Some relevant geometrical parameters describing the molecular shape and conformation are reported in Table 1.

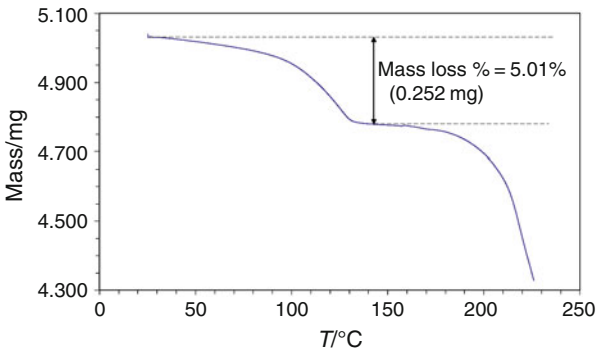

Fig. 3 TGA curve of NaIb monohydrate, obtained after pre-heating the sample in an oven at 80 °C for 5 min

Table 1 Selected geometrical parameters/Å,°

P(1)–O(2)	1.487(3)	Na···O(5)	2.306(4)	O(2)–P(1)–C(1)–P(2)	43.1(3)
P(1)–O(3)	1.517(3)	Na···O(2)	2.349(4)	O(3)–P(1)–C(1)–P(2)	169.5(2)
P(1)–O(4)	1.564(3)	Na···O(4)#2	2.351(4)	O(4)–P(1)–C(1)–P(2)	−75.6(3)
P(1)–C(1)	1.857(5)	Na···O(2)#3	2.408(4)	O(5)–P(2)–C(1)–P(1)	−74.2(3)
P(2)–O(5)	1.493(3)	Na···O(7)#2	2.458(4)	O(7)–P(2)–C(1)–P(1)	55.8(3)
P(2)–O(7)	1.498(3)	Na···O(1)#2	2.718(4)	O(6)–P(2)–C(1)–P(1)	171.6(2)
P(2)–O(6)	1.579(4)	Na···Na#3	3.397(4)		
P(2)–C(1)	1.847(5)				

Hydrogen bonding geometry/Å,°

D–H···A	d(D–H)	d(H···A)	d(D···A)	∠(DHA)
O(1)–H(1O)···O(3)#4	0.77(5)	1.95(6)	2.675(5)	157(5)
O(4)–H(4O)···O(7)#5	0.75(6)	1.81(6)	2.557(5)	175(6)
O(6)–H(6O)···O(1W)#1	0.79	1.99	2.692(6)	146.8
O(6)–H(6O)···O(1)	0.79	2.73	2.913(5)	95.2
N(1)–H(1N)···O(3)#6	0.99(5)	1.70(5)	2.690(5)	176(4)
O(1W)–H(2W)···O(5)	0.77	1.91	2.655(6)	163.7

Symmetry transformations used to generate equivalent atoms

#1 $x - 1, y, z$; #2 $x + 1, y, z$; #3 $-x + 1, -y, -z + 1$; #4 $-x, -y + 1, -z + 1$; #5 $-x, -y, -z + 1$; #6 $-x + 1, -y + 1, -z + 1$

The compound crystallizes with one water molecule for each anion–cation pair. The anionic moiety was found to exist as a zwitterion with an overall charge of −1: the protonated amine group bears a positive charge while each phosphonate group contains only one protonated oxygen atom thus resulting negatively charged. The zwitterionic form is a common feature for this type of bisphosphonates compounds (see for example: alendronate [1], monosodium olpadronate monohydrate [4], disodium pamidronate pentahydrate [5], risedronate monohydrate [7]) and gives reason for two distinct type of P–O bonds: (i) the P1–O4 and P2–O6 bond lengths (mean value 1.572(3) Å) are in agreement with single bond distances involving protonated O atoms, (ii) the other P–O distances (mean values 1.499(3) Å) show partial double bond character confirming a partial delocalization of the negative charge between the unprotonated O atoms. The geometry around each P atom corresponds to a slightly distorted tetrahedron, with four O–P–O bond angles in the range 106.9(2)° to 115.5(2)° and the O5–P2–O7 and O2–P1–O3 bond angles of 115.2(2)° and of 118.5(2)°, respectively. The aliphatic (alkylamine) chain is almost all *trans*, the larger deviation from planarity being due to the C2–C3–N1–C5 torsion angle [152.5(5)°]. The C3 atom is *trans* with respect to P1 atom [P1–C1–C2–C3 = 165.5(4)°] and gauche with respect to O1 atom [O1–C1–C2–C3 = 73.8(6)°].

The sodium cation is octahedrically coordinated to three different bisphosphonates units: in a tridentate fashion (through the O4 and O7 atoms and the hydroxyl O1 atom of the same unit), in a bidentate fashion (through the O2 and O5 atoms of a second unit) and in a monodentate fashion (through O2 atom of the third unit) (Fig. 4). The coordinating bond lengths Na···O involving phosphonate O atoms are in the range 2.306(4)–2.458(4) Å, while the Na···O1 distance is longer [2.717(4) Å]. As it has been found also for alendronate, the Na···O distances are not defined by the charge ascribed to the O atoms but could be correlated with packing interactions.

The coordination environment around Na cations results in a centrosymmetric double chains structure, running along the *a* axis (Fig. 5), in which the negative parts of the zwitterionic moieties are connected to the cations in the centre of the double chains while the alkylamine chains, positively charged, are elongated away in nearly parallel arrangement. Within the same chain the shortest Na···Na distances are 3.397(4) Å. This Na coordination environment and chain structure of the crystal packing is very similar to that found for sodium olpadronate and alendronate [1, 4].

The crystal packing is further completed by an extended network of intra and inter-chains hydrogen bonds defining an infinite two-dimensional structure in the *ab* plane. The water molecules are stacked in the [100] direction in the inter-chains cavities: each of them is connected as donor and as acceptor of hydrogen bonding to O5 and O6 atoms of the same double chain, respectively. This arrangement

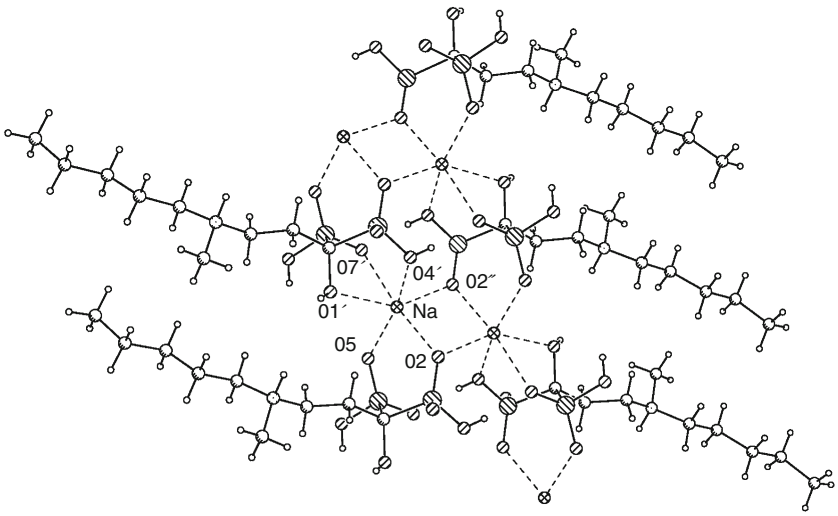

Fig. 4 Part of the crystal structure of NaIb monohydrate showing the octahedral coordination of the Na cations. For the sake of clarity, the H atoms have been omitted

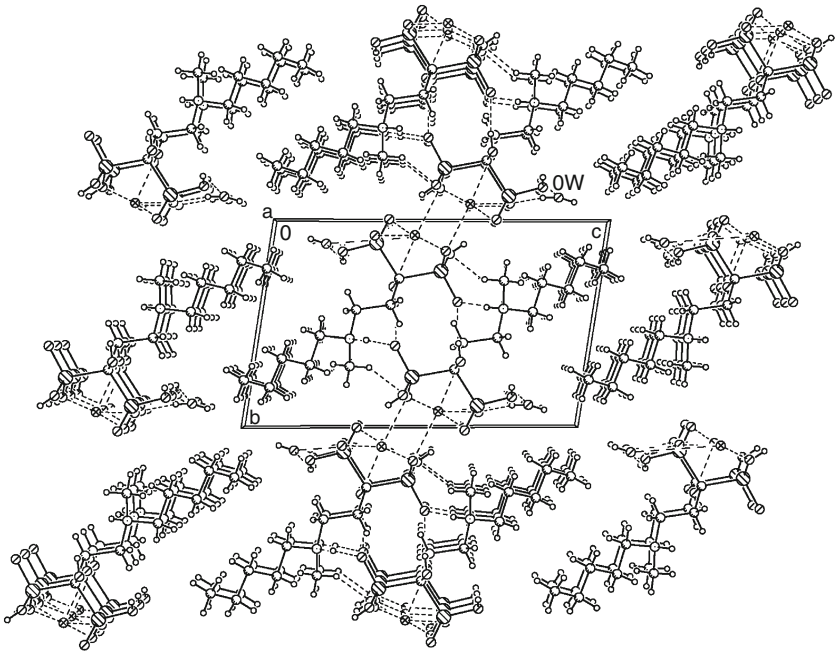

Fig. 5 The crystal packing of NaIb monohydrate viewed along the [100] direction, with the hydrogen bonds scheme. The position of a water molecule (Ow) is indicated

suggests that water molecules, even if hydrogen-bonded in the crystal packing, do not give a further significant contribution to its stability (vide infra).

Variable temperature X-ray powder diffraction

The high-temperature diffraction analysis was carried out in order to investigate the peculiarity of the thermal behaviour of the drug before the melting point, as observed on DSC diagram. The XRPD patterns, collected at increasing temperatures, show that no transition to other crystalline phases appears up to 150 °C, while a new phase is observed at 155 °C, that is just before the starting of the melting process (Fig. 6). The first well defined peaks of the X-ray powder diffraction pattern of this new phase, collected at 155 °C, were selected for the indexing procedure using TOPAS program [21] allowing the determination of the approximate cell parameters (lattice constants). Density consideration suggested the space group P-1 in the triclinic system, with two molecules in the unit cell. The lattice constants of this new phase are: $a = 5.932$ Å, $b = 9.110$ Å, $c = 16.437$ Å, $\alpha = 64.08°$, $\beta = 100.64°$, $\gamma = 93.98°$, $V = 785.2$ Å^3, $Z = 2$, $D_c = 1.519$ g cm^{-3}. The cell parameters are similar but significantly different from those determined by X-ray single crystal diffraction analysis at room temperature, indicating that a real phase transition occurred.

After the phase transition, the sample was cooled back to ambient temperature: the new phase disappeared and the drug re-crystallized in its starting crystalline phase,

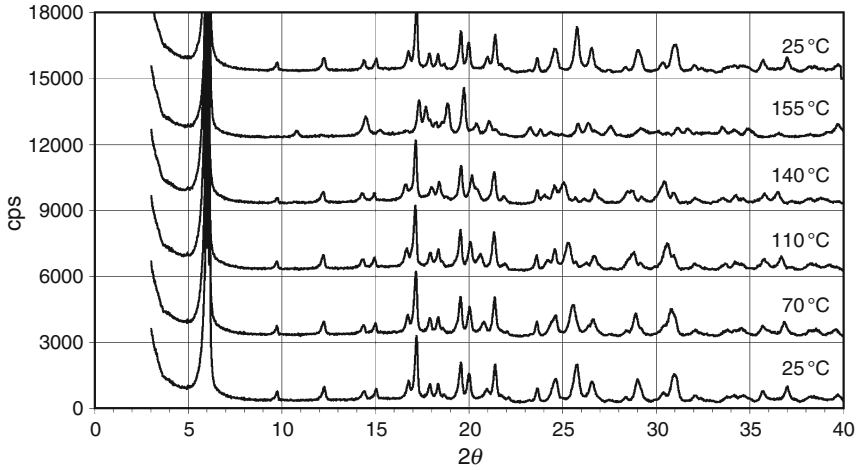

Fig. 6 X-ray powder diffraction patterns of the NaIb monohydrate, collected at different temperatures

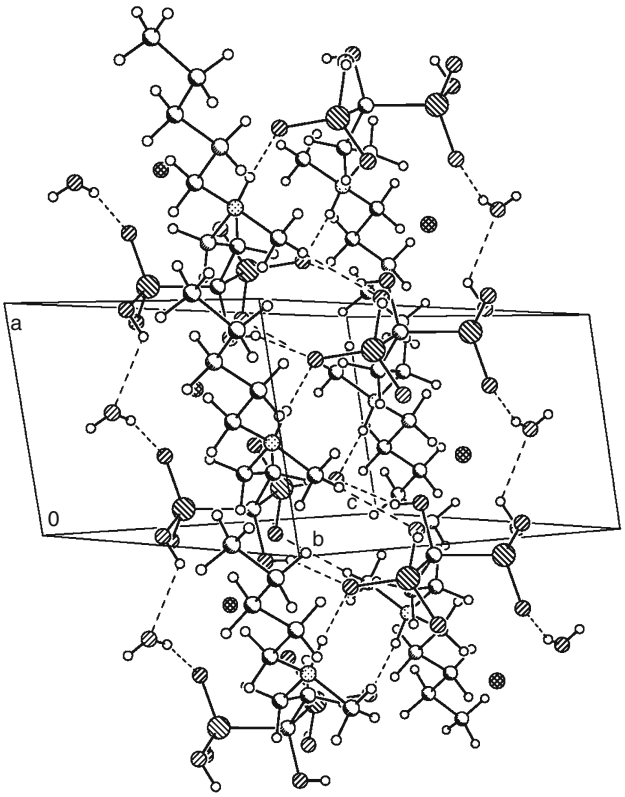

Fig. 7 An arbitrary view of part of the crystal packing of NaIb monohydrate, showing the formation of a double chain along [100] and the disposition of the water molecules on the lateral sides of the chain

confirming the metastable nature of the phase crystallized at 155 °C. This thermal behaviour suggests that NaIb monohydrate during the heating undergoes a solid–solid phase transition, due to a dehydration process, but, during the cooling, a rehydration process of the sample takes place. The rehydration event, due to the hygroscopic nature of the drug, could be interpreted on the basis of water arrangement observed in the crystal lattice: the water molecules are located inside the inter-chains cavities and are hydrogen-bonded on the lateral side of the crystalline backbone (Fig. 7) giving a poor contribution to its stability. The rehydration of the drug is favoured also by the experimental conditions, indeed the thermal chamber containing the sample during all the variable temperature diffraction analysis is maintained sealed, therefore no gas purge acts on the sample and the humidity released during the dehydration was not removed.

In a second thermodiffractometric experiment (X-ray diffraction pattern not reported), the drug was heated up to 180 °C to complete melting process and cooled back to ambient temperature: irreversible transition to an amorphous phase was observed.

Conclusions

Crystalline NaIb monohydrate appears to undergo thermal dehydration and rehydration processes that were monitored by variable temperature X-ray powder diffraction analysis.

Furthermore, thermogravimetric analysis shows a mass loss of 5% weight of the sample corresponding to a release of one water molecule per NaIb molecule.

The crystal structure of NaIb monohydrate was determined by means of single crystal X-ray analysis. The molecular geometry was fully determined and the molecular packing was investigated in order to clarify the stabilizing effects in the solid state. The NaIb crystallizes as monohydrate salt. Each anionic entity exists in form of zwitterionic unit with an overall charge of −1, the protonated amine group bearing a positive charge and each phosphonate group being negatively charged with only one O atom protonated. The crystal packing is determined by the octahedral coordination of the Na cations resulting in a centrosymmetric double chains structure, running parallel

to the crystallographic *a* axis. The solid state structure is further stabilized by an extended network of intra and inter-chains hydrogen bonds defining an infinite two-dimensional arrangement in the *ab* plane. The water molecules are located inside the inter-chains cavities and are hydrogen-bonded on the lateral side of each double chain (Fig. 7); this arrangement seems to not contribute significantly to the crystal packing, thus making possible the dehydration and rehydration processes which have been observed.

References

1. Vega D, Baggio R, Garland MT. Alendronate. Acta Cryst. 1996;C52:2198–201.
2. Martin MB, Grimley JS, Lewis JC, Heath HT, Bailey BN, Kendrick H, Yardley V, Caldera A, Lira R, Urbina JA, Moreno SNJ, Docampo R, Croft SL, Oldfield E. Bisphosphonates inhibit the growth of *Trypanosome brucei*, *Trypanosome cruzi*, *Leishmania donovani*, *Toxoplasma gondii* and *Plasmodium falciparum*. J Med Chem. 2001;44:909–16.
3. Fleisdch H. Development of bisphosphonates. Breast Cancer Res. 2002;4:30–4.
4. Vega D, Baggio R, Piro O. Monosodium Olpadronate monohydrate. Acta Cryst. 1998;C54:324–7.
5. Vega D, Fernandez D, Ellena JA. Disodium Pamidronate. Acta Cryst. 2002;C58:m77–80.
6. Fernandez D, Vega D, Ellena JA. Two members of bisphosphonate class of drugs: a zwitterion and a molecular compound. Acta Cryst. 2003;C59:o289–92.
7. Gossman WL, Wilson SR, Oldfield E. Three hydrates of the bisphosphonate risedronate, consisting of one molecular and two ionic structures. Acta Cryst. 2003;C59:m33–6.
8. Stahl K, Treppendahl SP, Preikscaht H, Fischer E. Sodium 3-ammonio-1-hydroxypropylidene-1,1-bisphosphonate monohydrate. Acta Cryst. 2005;E61:m132–4.
9. Rogers MJ. New insights into the molecular mechanisms of action of bisphosphonates. Curr Pharm Des. 2003;9:2643–58.
10. Eiermann U, Junghans B, Knipp B, Sattelkau T. Ibandronate polymorph B. WO2006081962A1.
11. Eiermann U, Junghans B, Knipp B, Sattelkau T. Ibandronate polymorph A. WO2006081963A1.
12. Pulla Reddy M, Usharani V, Venkaiah Chowdary, N. Novel Polymorphic forms of ibandronate. WO2007074475A3.
13. Szterner P, Legendre B, Sghaier M. Thermodynamic properties of polymorphic forms of theophylline. Part I: DSC, TG, X-ray study. J Therm Anal Calorim. 2010;99:325–35.
14. Malpezzi L, Fuganti C, Maccaroni E, Masciocchi N, Nardi A. Thermal and structural characterization of two polymorphs of Atovaquone and of its chloro derivative. J Therm Anal Calorim. 2010;102:203–10.
15. Drebushchak VA, Drebushchak TN, Chukanov NV, Boldyreva EV. Transition among five polymorphs of chloropropamide near the melting point. J Therm Anal Calorim. 2008;93:243–51.
16. Lee EA, Sohn YT. Crystal forms of a capsaicin derivative analgesic DAA-5018. J Therm Anal Calorim. 2008;93:871–4.
17. Gall R., Bosies E. Diphosphonate derivatives, pharmaceutical compositions and methods of use. US Patent 4,927,814 (1990).
18. Sheldrick GM. SADABS. Göttingen: University of Göttingen; 1996.
19. Altomare A, Burla MC, Camalli M, Cascarano GL, Giacovazzo C, Guagliardi A, Moliterni AGG, Polidori GP, Spagna R. SIR97: a new tool for crystal structure determination and refinement. J Appl Cryst. 1999;32:115–9.
20. Sheldrick GM. SHELXL-97, program for the refinement of crystal structures. Göttingen: University of Göttingen; 1997.
21. TOPAS-Academic. Version 4.1: Coelho Software. Brisbane: TOPAS-Academic; 2007.